SCIENTIFIC REPORTS

OPEN

Fast generation of W states of superconducting qubits with multiple Schrödinger dynamics

Yi-Hao Kang[1], Ye-Hong Chen[1], Qi-Cheng Wu[1], Bi-Hua Huang[1], Jie Song[2] & Yan Xia[1]

In this paper, we present a protocol to generate a W state of three superconducting qubits (SQs) by using multiple Schrödinger dynamics. The three SQs are respective embedded in three different coplanar waveguide resonators (CPWRs), which are coupled to a superconducting coupler (SCC) qubit at the center of the setups. With the multiple Schrödinger dynamics, we build a shortcuts to adiabaticity (STA), which greatly accelerates the evolution of the system. The Rabi frequencies of the laser pulses being designed can be expressed by the superpositions of Gaussian functions via the curves fitting, so that they can be realized easily in experiments. What is more, numerical simulation result shows that the protocol is robust against control parameters variations and decoherence mechanisms, such as the dissipations from the CPWRs and the energy relaxation. In addition, the influences of the dephasing are also resisted on account of the accelerating for the dynamics. Thus, the performance of the protocol is much better than that with the conventional adiabatic passage techniques when the dephasing is taken into account. We hope the protocol could be implemented easily in experiments with current technology.

Entanglement plays a significant role in quantum information processing (QIP)[1–12]. Therefore, the generation of entangled states for two or more particles is not only fundamental for showing quantum nonlocality[13–15], but also useful in many research fields in QIP, such as, quantum secure direct communication[16,17], quantum secret sharing[18,19], quantum teleportation[20,21], quantum cloning machine[22,23] and so on. For multi-qubit entanglement, there are two major types of entangled states, the W states[14] and the Greenberger-Horne-Zeilinger (GHZ) states[15], which can not be converted to each other by local operations and classical communications. The GHZ states are usually called as "maximally entangle" in several senses, e.g., the GHZ state violates Bell inequalities maximally. But a particle trace of a GHZ state results in a maximally mixed state compared with a nonmaximally mixed result for a W state, i.e., the W states show perfect correlations. Therefore, in past several years, the W states have attracted more attentions because of their robustness against qubit loss and advantages in quantum teleportation[20].

Till now, the generation of the W states has been studied in numerous systems[24–35], such as the atom-cavity coupled systems[24–26], electronic spin qubits inside the quantum dots systems[27], photons and linear optical systems[28,29], superconducting qubits (SQs) systems[30–36], etc. Among of these protocols[24–36], the generation of W states with SQs has shown fantastic advantages, since new progress in circuit cavity quantum electrodynamics makes it a standout performance among the most promising candidates for implementing QIP[37,38]. It has been shown that, the SQs (e.g., flux, phase and charge qubits) and microwave resonators can be manufactured using modern integrated circuit technology, their features can be characterized and adjusted *in situ*. Moreover, the SQs have relatively long decoherence times[39], and various single and multiple qubits operations with state readout have been shown[40–43]. Furthermore, a superconducting resonator can provide a quantized cavity field, in order that the fast and long-range interaction between distant SQs could be mediated[44–46]. What is more, it has been proved by both a lot of theoretical researches[47,48] and experiments[49,50] that, the strong-coupling limit can be easily realized with SQs. Therefore, creating W states with SQs is a wise choice.

On the other hand, if one decides to generate W states with SQs, another question is how to accurately controlling the system with high fidelity. Many previous researches have indicated that the adiabatic passages, especially the stimulated Raman scattering involving adiabatic passage (STIRAP) and its variants[51–54] hold robustness

[1]Department of Physics, Fuzhou University, Fuzhou 350002, China. [2]Department of Physics, Harbin Institute of Technology, Harbin 150001, China. Correspondence and requests for materials should be addressed to Y.X. (email: xia-208@163.com)

against variations of the controlled parameters. Generally speaking, if the system remains in the instantaneous ground state of its time-dependent Hamiltonian during the whole evolution process under an adiabatic control, the dissipations caused by decoherence, noise and losses may be repressed. However, we all know that, to prevent the transition between each instantaneous eigenstate, the adiabatic condition is required, which will badly limit the evolution speed of the system. During a long evolution, the dissipations may accumulate and finally destroy the intended dynamics. For example, refs 31 and 36 has shown that, the fidelity for generating of the W state by using adiabatic passage is quite sensitive to the dephasing, which is an ineluctable element of the decoherence mechanisms in the superconducting systems, i.e., a small increase of the dephasing rates causes a large decrease of the fidelity; this will also bring challenges to the experiments. Therefore, to overcome the problem causing by the long evolution time of the adiabatic passage, one should speed up the evolution by using some other techniques. To speed up the evolution, using resonant interaction is a choice. But unfortunately, using resonant interaction will make the system quite sensitive to the variations of experimental parameters. For example, if there are a little variations of the evolution time or Rabi frequencies of laser pulses, the fidelity will decrease a lot. It is also proved in ref. 32 that, with resonant interaction, the population of each state changes rapidly when the evolution time increases, and a high fidelity of the target state only appears in very narrow ranges around some certain moments. Therefore, methods with both robustness and high speed are desired, and consequently, a new technique called "Shortcuts to adiabatic passage" (STAP) has been proposed[55-63].

The STAP is closely related to adiabatic passage but totally breaks the limit of the adiabatic condition. It depicts a rapid adiabatic-like process which is not really adiabatic but leading to the same goals with adiabatic process. With these advantages, the STAP has attracted a lot of interests and been used in many research fields including "fast cold-atom", "fast ion transport", "fast quantum information processing", "fast wave-packet splitting", "fast expansion", and so on refs 64–93. Among of these protocols[55-93], the method named "Transitionless quantum driving" (TQD)[58-61] has shown its power to construct the STAP. However, when we accelerate adiabatic protocols using TQD, the structure or the values of the shortcut-driving Hamiltonian might not exist in practice. For example, in refs 24,80,94–96, the authors did a lot to design Hamiltonians to overcome the problem caused by the problematic terms which are actually equivalent to the special one-photon 1–3 pulse (the microwave field). Nevertheless, the operations usually cause some other problems or make some other limiting conditions to the protocols, for examples, there will be a limiting condition for the total operation time to generate the entangled states. Therefore, numerous protocols with different methods[97-107] have been further presented to avoid the problematic terms of the system's Hamiltonian which is designed by TQD. Among of these methods[97-107], the multiple Schrödinger dynamics[104,105] is a very interesting method. It exploits iterative interaction pictures to obtain Hamiltonians with physically feasible structure for quantum systems. Moreover, by choosing suitable boundary conditions, it enables the designed interaction picture to reproduce the same final population (or state) as those in the original Schrödinger picture. In 2012, Ibáñez et al.[105] have adopted some Schrödinger pictures and dynamics to design alternative and feasible STAP for harmonic transport, trap expansions and trap compressions. Subsequently, in 2013, Ibáñez et al.[104] have studied the capabilities and limitations of superadiabatic iterations to construct a sequence of shortcuts to adiabaticity by iterative interaction pictures. Afterwards, Song et al.[106] have investigated the physical feasibility of the multiple Schrödinger dynamics in a three-level systems, and obtained very interesting results in 2016. They have shown that the Hamiltonian of the interaction picture in the second iteration has the same form as the Hamiltonian in the original Schrödinger picture. This makes the multiple Schrödinger dynamics useful in three-level systems.

Inspired by the protocols in refs 104–106, as well as considering the advantages of the superconducting systems, we come up with a protocol for generating a W state of three SQs by using multiple Schrödinger dynamics. With the help of the multiple Schrödinger dynamics, a STAP is constructed, which greatly speeds up the evolution of the system. The Hamiltonian being designed in this protocol has the same form as the system's original Hamiltonian. Moreover, the Rabi frequencies of the laser pulses being designed can be expressed by the superpositions of Gaussian functions assisted by the curves fitting, so that they can be realized in experiments. Numerical simulation demonstrates that the protocol is robust against control parameters variations and decoherence mechanisms, such as the dissipations from the coplanar waveguide resonators (CPWRs) and the energy relaxation of SQs. What is more, the influences of the dephasing are also resisted because of the accelerating for the dynamics. Therefore, the performance of the protocol is much better comparing with the conventional adiabatic passage techniques when the dephasing is taken into account. Based on a circuit quantum electrodynamics system, the protocol could be controlled and implemented readily in experiments.

The article is organized as follows. In the section of "The multiple Schrödinger dynamics", we will introduce the method of the multiple Schrödinger dynamics. In the section of "Fast generation of W states of superconducting qubits with multiple Schrödinger dynamics", we will describe the generation of a W state of three SQs in detail. In the section of "Numerical simulations and discussions", we will investigate the performance of the protocol when the control parameters variations and decoherence mechanisms are considered. Finally, the conclusions will be given in the section of "Conclusions".

The multiple Schrödinger dynamics

In this section, we would like to review the multiple Schrödinger dynamics[104–106] firstly. Assume that the original Hamiltonian of the system is $H_0(t)$. We perform a picture transformation as $|\psi_1(t)\rangle = A_0^\dagger(t)|\psi_0(t)\rangle$, where $A_0(t) = \sum_n |n_0(t)\rangle\langle n_0(0)|$ and $|n_0(t)\rangle$ is the n-th instantaneous eigenstate of $H_0(t)$. So, the Hamiltonian in the 1-st interaction picture is $H_1(t) = A_0^\dagger(t)[H_0(t) - K_0(t)]A_0(t)$ with $K_0(t) = i\dot{A}_0(t)A_0^\dagger(t)$. Suppose that the 1-st modified Schrödinger Hamiltonian is $H_0^{(1)}(t) = H_0(t) + H_{cd}^{(0)}$. If one hopes the transitions between instantaneous eigenstates $\{|n_0(t)\rangle\}$ are all forbidden, the simplest choice is $H_{cd}^{(0)} = K_0$, so that the Hamiltonian in the 1-st interaction picture is diagonal. If the 1-st modified Hamiltonian $H_0^{(1)}(t)$ is difficult to be realized, the 2-nd interaction
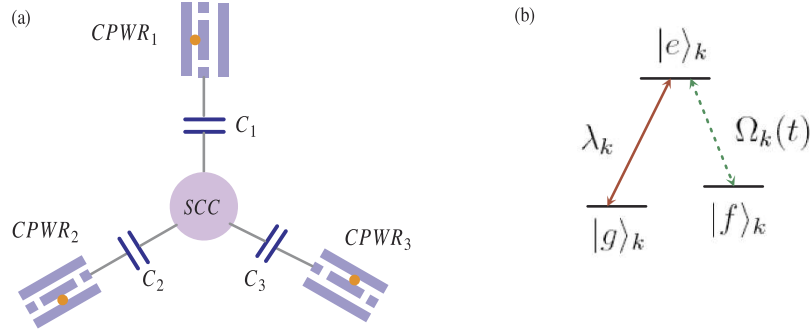
Figure 1. (**a**) Schematic diagram of three CPWRs and a SCC qubit (a circle at the center). (**b**) The energy-level structure of SQ_k.

picture should be introduced. Assume that $\{|n_1(t)\rangle\}$ are the eigenstates of $H_1(t)$. We perform a picture transformation as $|\psi_2(t)\rangle = A_1^\dagger(t)|\psi_1(t)\rangle$ with $A_1(t) = \sum_n |n_1(t)\rangle\langle n_1(0)|$. Then, we obtain the Hamiltonian in the 2-nd interaction picture as $H_2(t) = A_1^\dagger(t)[H_1(t) - K_1(t)]A_1(t)$ with $K_1(t) = i\dot{A}_1(t)A_1^\dagger(t)$. Suppose that the 2-nd modified Schrödinger Hamiltonian is $H_0^{(2)}(t) = H_0(t) + H_{cd}^{(1)}$. To forbid the transitions between $\{|n_1(t)\rangle\}$ and diagonalize the Hamiltonian in the 2-nd interaction picture, $H_{cd}^{(1)}$ can be calculated as $H_{cd}^{(1)} = A_0(t)K_1(t)A_0^\dagger(t)$. Repeating the processing as the 1-st and the 2-nd iterations, according to the Hamiltonian in the j-th ($j \in \{1, 2, 3, ..., N\}$) interaction picture ($H_j(t)$), one can obtain the j-th modified Schrödinger Hamiltonian as

$$H_0^{(j)}(t) = H_0(t) + H_{cd}^{(j-1)} = H_0(t) + iB_j(t)\dot{A}_j(t)A_j^\dagger(t)B_j^\dagger(t), \tag{1}$$

where $B_j(t) = A_0(t)A_1(t)\cdots A_{j-1}(t)$ and $A_j(t) = \sum_n |n_j(t)\rangle\langle n_j(0)|$ with $\{|n_j(t)\rangle\}$ being the instantaneous eigenstates of $H_j(t)$. Governed by the Hamiltonian $H_0^{(j)}(t)$, the transitions between instantaneous eigenstates $\{|n_j(t)\rangle\}$ of H_j are forbidden.

Fast generation of W states of superconducting qubits with multiple Schrödinger dynamics

In this section, we will show how to generate a W state of three SQs with multiple Schrödinger dynamics. Consider a system composed of a superconducting coupler (SCC) qubit and three CPWRs ($CPWR_1$, $CPWR_2$ and $CPWR_3$). As shown in Fig. 1(a), the SCC qubit in the center of the devices is coupled to $CPWR_k$ through capacitor C_k ($k \in \{1, 2, 3\}$). There is a SQ named SQ_k in the $CPWR_k$, which has an excited state $|e\rangle_k$ and two ground states $|g\rangle_k$ and $|f\rangle_k$. As shown in Fig. 1(b) the transition $|e\rangle_k \leftrightarrow |f\rangle_k$ is driven by the laser pulse with Rabi frequency $\Omega_k(t)$, and the transition $|e\rangle_k \leftrightarrow |g\rangle_k$ is coupled to $CPWR_k$ with coupling constant λ_k. As for the SCC qubit, it has an excited state $|e\rangle_c$ and two ground states $|g\rangle_c$ and $|f\rangle_c$, which has similar structure as the three SQs. The transition $|e\rangle_c \leftrightarrow |f\rangle_c$ is driven by the laser pulse with Rabi frequency $\Omega_c(t)$. Different from the three SQs, the transition $|e\rangle_c \leftrightarrow |g\rangle_c$ may couple to three CPWRs with different coupling constants. We assume that the coupling constant for the transition $|e\rangle_c \leftrightarrow |g\rangle_c$ coupled to $CPWR_k$ is ν_k. Therefore, in the interaction picture, the Hamiltonian for the system can be written by

$$H_I(t) = H_c + H_l(t),$$
$$H_c = \sum_{k=1}^{3} \lambda_k a_k |e\rangle_k\langle g| + \sum_{k=1}^{3} \nu_k a_k |e\rangle_c\langle g| + H.c.,$$
$$H_l(t) = \Omega_c(t)|e\rangle_c\langle f| + \sum_{k=1}^{3} \Omega_k(t)|e\rangle_k\langle f| + H.c. \tag{2}$$

For simplicity of calculations, we adopt $\lambda_k = \lambda$ and $\nu_k = \nu$ in the following. Assuming that the initial state of the system is $|\Psi(0)\rangle = |f\rangle_r|g\rangle_1|g\rangle_2|g\rangle_3|0\rangle_1|0\rangle_2|0\rangle_3$, where, $|0\rangle_k$ and $|1\rangle_k$ are the vacuum state and one-photon state of the cavity mode in k-th CPWR, respectively. The excited number operator of the system is defined by $N_e = |e\rangle_c\langle e| + |f\rangle_c\langle f| + \sum_n(|e\rangle_k\langle e| + |f\rangle_k\langle f| + a_j^\dagger a_j)$. As $[N_e, H_I] = 0$, and $\langle\Psi(0)|N_e|\Psi(0)\rangle = 1$, the system will remain in the one-excited subspace spanned by

$$|\varphi_1\rangle = |f\rangle_c|g\rangle_1|g\rangle_2|g\rangle_3|0\rangle_1|0\rangle_2|0\rangle_3, \quad |\varphi_2\rangle = |e\rangle_c|g\rangle_1|g\rangle_2|g\rangle_3|0\rangle_1|0\rangle_2|0\rangle_3,$$
$$|\varphi_3\rangle = |g\rangle_c|g\rangle_1|g\rangle_2|g\rangle_3|1\rangle_1|0\rangle_2|0\rangle_3, \quad |\varphi_4\rangle = |g\rangle_c|g\rangle_1|g\rangle_2|g\rangle_3|0\rangle_1|1\rangle_2|0\rangle_3,$$
$$|\varphi_5\rangle = |g\rangle_c|g\rangle_1|g\rangle_2|g\rangle_3|0\rangle_1|0\rangle_2|1\rangle_3, \quad |\varphi_6\rangle = |g\rangle_c|e\rangle_1|g\rangle_2|g\rangle_3|0\rangle_1|0\rangle_2|0\rangle_3,$$
$$|\varphi_7\rangle = |g\rangle_c|g\rangle_1|e\rangle_2|g\rangle_3|0\rangle_1|0\rangle_2|0\rangle_3, \quad |\varphi_8\rangle = |g\rangle_c|g\rangle_1|g\rangle_2|e\rangle_3|0\rangle_1|0\rangle_2|0\rangle_3,$$
$$|\varphi_9\rangle = |g\rangle_c|f\rangle_1|g\rangle_2|g\rangle_3|0\rangle_1|0\rangle_2|0\rangle_3, \quad |\varphi_{10}\rangle = |g\rangle_c|g\rangle_1|f\rangle_2|g\rangle_3|0\rangle_1|0\rangle_2|0\rangle_3,$$
$$|\varphi_{11}\rangle = |g\rangle_c|g\rangle_1|g\rangle_2|f\rangle_3|0\rangle_1|0\rangle_2|0\rangle_3. \tag{3}$$

Moreover, the eigenstates of H_c can be described as

$$|\phi_0\rangle = \frac{1}{\sqrt{\lambda^2 + 3\nu^2}}[\lambda|\varphi_2\rangle - \nu(|\varphi_6\rangle + |\varphi_7\rangle + |\varphi_8\rangle)],$$

$$|\phi_1\rangle = \frac{1}{2}(|\varphi_3\rangle - |\varphi_5\rangle + |\varphi_6\rangle - |\varphi_8\rangle),$$

$$|\phi_2\rangle = \frac{1}{2}(|\varphi_3\rangle - |\varphi_4\rangle + |\varphi_6\rangle - |\varphi_7\rangle),$$

$$|\phi_3\rangle = \frac{1}{2}(|\varphi_3\rangle - |\varphi_5\rangle - |\varphi_6\rangle + |\varphi_8\rangle),$$

$$|\phi_4\rangle = \frac{1}{2}(|\varphi_3\rangle - |\varphi_4\rangle - |\varphi_6\rangle + |\varphi_7\rangle),$$

$$|\phi_5\rangle = \frac{1}{\sqrt{6}}\left[\frac{3\nu}{\sqrt{\lambda^2 + 3\nu^2}}|\varphi_2\rangle + |\varphi_3\rangle + |\varphi_4\rangle + |\varphi_5\rangle\right.$$

$$\left. +\frac{\lambda}{\sqrt{\lambda^2 + 3\nu^2}}(|\varphi_6\rangle + |\varphi_7\rangle + |\varphi_8\rangle)\right],$$

$$|\phi_6\rangle = \frac{1}{\sqrt{6}}\left[\frac{3\nu}{\sqrt{\lambda^2 + 3\nu^2}}|\varphi_2\rangle - |\varphi_3\rangle - |\varphi_4\rangle - |\varphi_5\rangle\right.$$

$$\left. +\frac{\lambda}{\sqrt{\lambda^2 + 3\nu^2}}(|\varphi_6\rangle + |\varphi_7\rangle + |\varphi_8\rangle)\right],$$

$$(4)$$

with corresponding eigenvalues $\varepsilon_0 = 0$, $\varepsilon_1 = \lambda$, $\varepsilon_2 = \lambda$, $\varepsilon_3 = -\lambda$, $\varepsilon_4 = -\lambda$, $\varepsilon_5 = \sqrt{\lambda^2 + 3\nu^2}$ and $\varepsilon_6 = -\sqrt{\lambda^2 + 3\nu^2}$, respectively.

For simplicity, we set $\Omega_1(t) = \Omega_2(t) = \Omega_3(t) = \sqrt{2}\Omega_a(t)$ and $\Omega_c(t) = \sqrt{2}\Omega_b(t)$. Under the condition $\Omega_a(t)$, $\Omega_b(t) \ll \lambda, \nu$, we can obtain the effective Hamiltonian of the system as

$$H_{eff}(t) = \frac{\sqrt{2}\lambda\Omega_b(t)}{\sqrt{\lambda^2 + 3\nu^2}}|\varphi_1\rangle\langle\phi_0| - \frac{\sqrt{2}\nu\Omega_a(t)}{\sqrt{\lambda^2 + 3\nu^2}}(|\varphi_9\rangle + |\varphi_{10}\rangle + |\varphi_{11}\rangle)\langle\phi_0| + H.c.$$

$$= \sqrt{2}\Omega_b(t)\cos\alpha|\varphi_1\rangle\langle\phi_0| - \sqrt{2}\Omega_a(t)\sin\alpha|W\rangle\langle\phi_0| + H.c., \quad (5)$$

where $\cos\alpha = \frac{\lambda}{\sqrt{\lambda^2 + 3\nu^2}}$, $\sin\alpha = \frac{\sqrt{3}\nu}{\sqrt{\lambda^2 + 3\nu^2}}$, $|W\rangle = \frac{1}{\sqrt{3}}(|\varphi_9\rangle + |\varphi_{10}\rangle + |\varphi_{11}\rangle)$. Without loss the generality, we assume $\alpha = \pi/4$. We also assume $\Omega(t) = \sqrt{\Omega_b^2(t) + \Omega_a^2(t)}$ and $\theta(t) = \arctan[\Omega_b(t)/\Omega_a(t)]$. Then, the system's effective Hamiltonian can be written by

$$H_{eff}(t) = \Omega(t)(\sin\theta|\varphi_1\rangle\langle\phi_0| - \cos\theta|W\rangle\langle\phi_0|) + H.c. \quad (6)$$

Afterwards, the instantaneous eigenstates of $H_{eff}(t)$ can be solved as

$$|\xi_0(t)\rangle = \cos\theta|\varphi_1\rangle + \sin\theta|W\rangle,$$

$$\left|\xi_+(t)\right\rangle = \frac{1}{\sqrt{2}}(\sin\theta|\varphi_1\rangle + |\phi_0\rangle - \cos\theta|W\rangle),$$

$$|\xi_-(t)\rangle = \frac{1}{\sqrt{2}}(\sin\theta|\varphi_1\rangle - |\phi_0\rangle - \cos\theta|W\rangle), \quad (7)$$

with corresponding eigenvalues $\epsilon_0 = 0$, $\epsilon_+ = \Omega$ and $\epsilon_- = -\Omega$, respectively. Therefore, the picture transformation for the 1-st iteration in basis $\{|\varphi_1\rangle, |\phi_0\rangle, |W\rangle\}$ is

$$A_0 = \begin{bmatrix} \cos\theta & \sin\theta/\sqrt{2} & \sin\theta/\sqrt{2} \\ 0 & 1/\sqrt{2} & -1/\sqrt{2} \\ \sin\theta & -\cos\theta/\sqrt{2} & -\cos\theta/\sqrt{2} \end{bmatrix}. \quad (8)$$

By calculating $H_{cd}^{(0)} = i\dot{A}(t)A^\dagger(t)$, in basis $\{|\varphi_1\rangle, |\phi_0\rangle, |W\rangle\}$, we obtain

$$H_{cd}^{(0)}(t) = \begin{bmatrix} 0 & 0 & i\dot{\theta} \\ 0 & 0 & 0 \\ -i\dot{\theta} & 0 & 0 \end{bmatrix}. \quad (9)$$

If we add $H_{cd}^{(0)}$ to modify the Hamiltonian $H_{eff}(t)$ in Eq. (6), the structure of the system is also required to be adjusted. Therefore, we consider the 2-nd iteration picture to find another shortcut. Then, the Hamiltonian in the 1-st iteration picture can be solved in basis $\{|\xi_0\rangle, |\xi_+\rangle, |\xi_-\rangle\}$ as

$$H_1(t) = \begin{bmatrix} 0 & i\dot{\theta}/\sqrt{2} & i\dot{\theta}/\sqrt{2} \\ -i\dot{\theta}/\sqrt{2} & \Omega & 0 \\ -i\dot{\theta}/\sqrt{2} & 0 & -\Omega \end{bmatrix}. \tag{10}$$

Defining $P = \Omega + \sqrt{\Omega^2 + \dot{\theta}^2}$, $Q = -\Omega + \sqrt{\Omega^2 + \dot{\theta}^2}$ and $R = 2\sqrt{\Omega^2 + \dot{\theta}^2}$, the eigenstates of $H_1(t)$ can be described as

$$\begin{aligned} |\Xi_0(t)\rangle &= (2\Omega|\xi_0\rangle + i\sqrt{2}\dot{\theta}|\xi_+\rangle - i\sqrt{2}\dot{\theta}|\xi_-\rangle)/R, \\ |\Xi_+(t)\rangle &= (i\sqrt{2}\dot{\theta}|\xi_0\rangle + P|\xi_+\rangle + Q|\xi_-\rangle)/R, \\ |\Xi_-(t)\rangle &= (i\sqrt{2}\dot{\theta}|\xi_0\rangle - Q|\xi_+\rangle - P|\xi_-\rangle)/R, \end{aligned} \tag{11}$$

corresponding to the eigenvalues $\eta_0 = 0, \eta_+ = \sqrt{\Omega^2 + \dot{\theta}^2}$ and $\eta_- = -\sqrt{\Omega^2 + \dot{\theta}^2}$, respectively. Therefore, the picture transformation for the 2-nd iteration in basis $\{|\xi_0\rangle, |\xi_+\rangle, |\xi_-\rangle\}$ can be given by

$$A_1 = \frac{1}{R} \begin{bmatrix} 2\Omega & i\sqrt{2}\dot{\theta} & i\sqrt{2}\dot{\theta} \\ i\sqrt{2}\dot{\theta} & P & -Q \\ -i\sqrt{2}\dot{\theta} & Q & -P \end{bmatrix}. \tag{12}$$

Submitting $j = 2$, Eqs (6) and (12) into Eq. (1), one can obtain the 2-nd modified Hamiltonian for $H_{eff}(t)$ in basis $\{|\varphi_1\rangle, |\phi_0\rangle, |W\rangle\}$ as

$$\begin{aligned} H_{eff}^{(2)}(t) &= \begin{bmatrix} 0 & \Omega\sin\theta - \Upsilon\cos\theta & 0 \\ \Omega\sin\theta - \Upsilon\cos\theta & 0 & \Omega\cos\theta + \Upsilon\sin\theta \\ 0 & \Omega\cos\theta + \Upsilon\sin\theta & 0 \end{bmatrix} \\ &= \begin{bmatrix} 0 & \widetilde{\Omega}_b & 0 \\ \widetilde{\Omega}_b & 0 & \widetilde{\Omega}_a \\ 0 & \widetilde{\Omega}_a & 0 \end{bmatrix}, \end{aligned} \tag{13}$$

where $\Upsilon = 4(\dot{\Omega}\dot{\theta} - \Omega\ddot{\theta})/R^2$, $\dot{\Omega} = (\Omega_b\dot{\Omega}_b + \Omega_a\dot{\Omega}_a)/\Omega$, $\ddot{\theta} = [(\ddot{\Omega}_b\Omega_a - \Omega_b\ddot{\Omega}_a)\Omega - 2\dot{\Omega}(\dot{\Omega}_b\Omega_a - \Omega_b\dot{\Omega}_a)]/\Omega^3$, $\widetilde{\Omega}_b = \Omega_b - \Upsilon\cos\theta$ and $\widetilde{\Omega}_a = \Omega_a + \Upsilon\sin\theta$. We find that $H_{eff}^{(2)}(t)$ has the same form as $H_{eff}(t)$. Therefore, using $H_{eff}^{(2)}(t)$ instead of $H_{eff}(t)$, we only need to adjust the Rabi frequencies $\Omega_b(t)$ and $\Omega_a(t)$.

Now, let us design the frequencies $\Omega_b(t)$ and $\Omega_a(t)$ so that the system governed by $H_{eff}^{(2)}(t)$ can be driven from its initial state $|\Psi(0)\rangle = |\varphi_1\rangle$ to the target state $|W\rangle$. Firstly, when the system is governed by $H_{eff}^{(2)}(t)$, the transitions between instantaneous eigenstates $\{|\Xi_0\rangle, |\Xi_+\rangle, |\Xi_-\rangle\}$ of $H_1(t)$ are forbidden. Assuming that the initial time is $t_i = 0$ and the final time is $t_f = T$, we find that if the boundary condition $\dot{\theta}(0) = \dot{\theta}(T) = 0$ is satisfy, the instantaneous eigenstate $|\Xi_0(t)\rangle$ of H_1 will coincide with the dark state $|\xi_0(t)\rangle$ of $H_{eff}(t)$ at $t = 0$ and $t = T$. Therefore, we adopt the boundary condition $\dot{\theta}(0) = \dot{\theta}(T) = 0$, and we set $\theta(0) = 0$ and $\theta(T) = \pi/2$. Then, we will have the following results

$$\begin{aligned} |\Psi(0)\rangle &= |\Xi_0(0)\rangle = |\xi_0(0)\rangle = |\varphi_1\rangle, \\ |\Psi(T)\rangle &= |\Xi_0(T)\rangle = |\xi_0(T)\rangle = |W\rangle. \end{aligned} \tag{14}$$

So, the system will evolve along the instantaneous eigenstate $|\Xi_0(t)\rangle$ of H_1 and finally at $t = T$, we can obtain the target state $|\Psi(T)\rangle = |W\rangle$. After the boundary conditions of θ and $\dot{\theta}$ are set, in the second step, let us design the Rabi frequencies of the laser pulses. To satisfy the boundary conditions of θ and $\dot{\theta}$ mentioned above, we firstly design the Ω_b and Ω_a via STIRAP. Ω_b and Ω_a can be expressed as

$$\Omega_b(t) = \Omega_0 e^{-[(t - t0 - T/2)/t_c]^2}, \quad \Omega_a(t) = \Omega_0 e^{-[(t + t0 - T/2)/t_c]^2}, \tag{15}$$

where Ω_0 is the pulse amplitude, $t_0 = 0.16T$ and $t_c = 0.25T$ are two related parameters. By calculating $\widetilde{\Omega}_b = \Omega_b - \Upsilon\cos\theta$ and $\widetilde{\Omega}_a = \Omega_a + \Upsilon\sin\theta$, one can obtain the Rabi frequencies $\widetilde{\Omega}_b$ and $\widetilde{\Omega}_a$ of laser pulses for the modified Hamiltonian $H_{eff}^{(2)}(t)$. However, the forms of $\widetilde{\Omega}_b$ and $\widetilde{\Omega}_a$ are too complex to be realized in experiments. For the sake of making the protocol more feasible in experiments, the Rabi frequencies of laser pulses should be expressed by some frequently used functions (e.g. Gaussian functions and sine function), or their superpositions. Fortunately, by using curves fitting, $\widetilde{\Omega}_b$ and $\widetilde{\Omega}_a$ can be replaced respectively with $\overline{\Omega}_b$ and $\overline{\Omega}_a$, whose expressions can be written by

$$\begin{aligned} \overline{\Omega}_b(t) &= \zeta_{b_1} e^{-\left[(t - \tau_{b_1})/\chi_{b_1}\right]^2} + \zeta_{b_2} e^{-\left[(t - \tau_{b_2})/\chi_{b_2}\right]^2}, \\ \overline{\Omega}_a(t) &= \zeta_{a_1} e^{-\left[(t - \tau_{a_1})/\chi_{a_1}\right]^2} + \zeta_{a_2} e^{-\left[(t - \tau_{a_2})/\chi_{a_2}\right]^2}, \end{aligned} \tag{16}$$
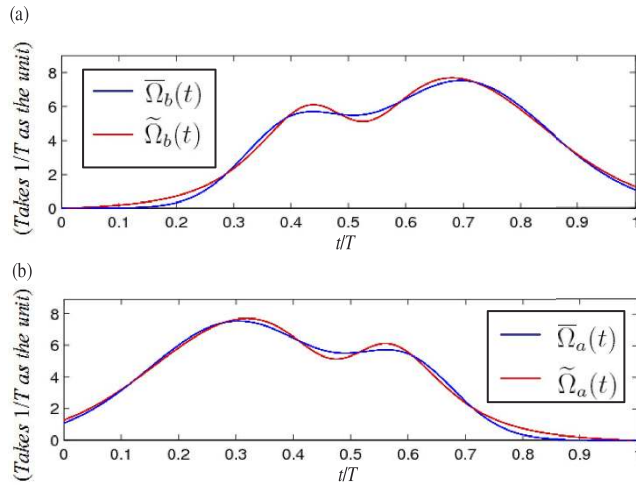
Figure 2. (**a**) Comparison between $\widetilde{\Omega}_b(t)$ and $\overline{\Omega}_b(t)$ (versus t/T). (**b**) Comparison between $\widetilde{\Omega}_a(t)$ and $\overline{\Omega}_a(t)$ (versus t/T).
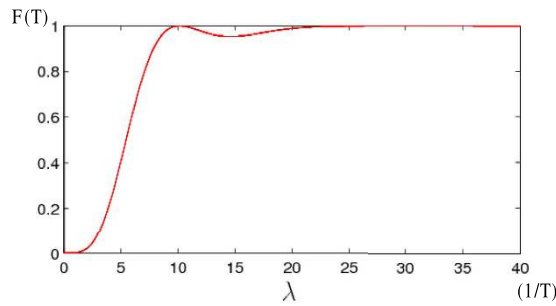
Figure 3. The final fidelity $F(T)$ versus λ.

where,

$$\zeta_{b_1} = 7.513/T, \quad \zeta_{b_2} = 4.3/T, \qquad \zeta_{a_1} = 7.513/T, \quad \zeta_{a_2} = 4.3/T,$$
$$\tau_{b_1} = 0.697T, \quad \tau_{b_2} = 0.4T, \qquad \tau_{a_1} = 0.303T, \quad \tau_{a_2} = 0.6T,$$
$$\chi_{b_1} = 0.217T, \quad \chi_{b_2} = 0.1222T, \quad \chi_{a_1} = 0.217T, \quad \chi_{a_2} = 0.1222T, \tag{17}$$

when $\Omega_0 = 8/T$. As a comparison, we plot $\widetilde{\Omega}_b(t)$ and $\overline{\Omega}_b(t)$ versus t/T in Fig. 2(a) and $\widetilde{\Omega}_a(t)$ and $\overline{\Omega}_a(t)$ versus t/T in Fig. 2(b). As shown in Fig. 2, the curve for $\overline{\Omega}_b(t)$ $(\overline{\Omega}_a(t))$ is very close to that for $\widetilde{\Omega}_b(t)$ $(\widetilde{\Omega}_a(t))$. In the next section, we will show that the laser pulses with Rabi frequencies $\overline{\Omega}_1(t) = \sqrt{2} \times \overline{\Omega}_b(t)$, $\overline{\Omega}_2(t) = \sqrt{2} \times \overline{\Omega}_b(t)$, $\overline{\Omega}_3(t) = \sqrt{2} \times \overline{\Omega}_b(t)$ and $\overline{\Omega}_c(t) = \sqrt{2} \times \overline{\Omega}_a(t)$ can drive the system from its initial state $|\Psi(0)\rangle = |\varphi_1\rangle$ to the target state $|\Psi(T)\rangle = |W\rangle$ with a high fidelity, so, the replacements here for the Rabi frequencies of the laser pulses are effective.

Numerical Simulations and Discussions

In this section, various numerical simulations will be performed to demonstrate the effective of the present protocol. The fidelity of the target state $|W\rangle$ is defined as $F(t) = |\langle W|\rho(t)|W\rangle|$, where $\rho(t)$ is the density operator of the system. Firstly, let us choose suitable coupling constants λ and ν. As we adopted $\alpha = \pi/4$, the relation between λ and ν is $\lambda = \sqrt{3}\nu$. And the Rabi frequencies of laser pulses satisfy $\overline{\Omega}_0 = \max_{0 \leq t \leq T} \{\overline{\Omega}_1(t), \overline{\Omega}_2(t), \overline{\Omega}_3(t), \overline{\Omega}_c(t)\} \approx 12/T$.

We plot the final fidelity $F(T)$ versus λ in Fig. 3. As shown in Fig. 3, $F(T)$ is near 1 around $\lambda = 10/T$. Moreover, $F(t)$ is close to 1 when $\lambda > 20/T$. One can easily find that even when the condition $\overline{\Omega}_a(t), \overline{\Omega}_b(t) \ll \lambda$, ν is not satisfied well, the target state $|W\rangle$ can also be obtained. This can also easily be understood, as the evolution of the system, between the initial state $|\varphi_1\rangle$ and the target state $|W\rangle$, may move along different medium states, and it is not governed by the effective Hamiltonian $H_{eff}(t)$, which guides the system moving through the dark state $|\phi_0\rangle$ of H_c as the only medium state. However, when the condition $\overline{\Omega}_a(t), \overline{\Omega}_b(t) \ll \lambda$, ν is broken, the system may move through a medium state with higher energy. That will make the evolution of the system suffers more from dissipations. On the other hand, for a relative higher evolution speed, the value of λT should not be too large, as λ has a upper limit
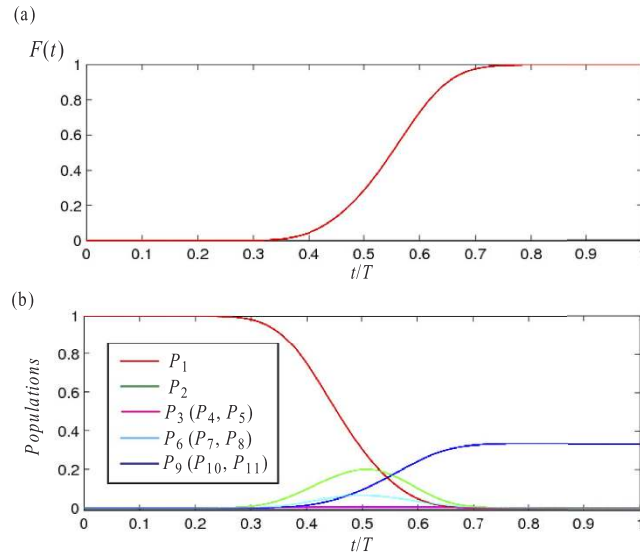
(a)

(b)

Figure 4. (**a**) The fidelity $F(t)$ versus t/T. (**b**) The population P_m of $|\varphi_m\rangle$ versus t/T.
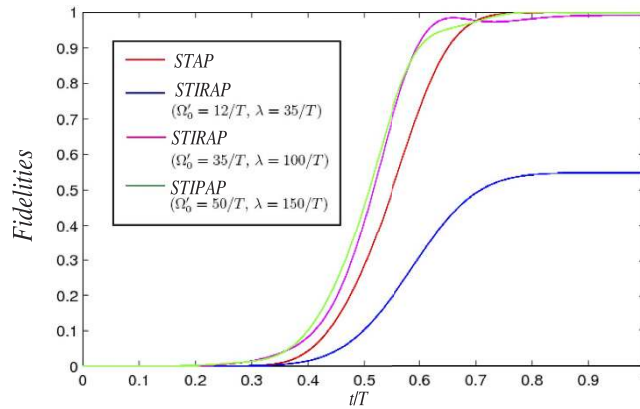

Figure 5. The fidelities of the target state $|W\rangle$ versus t/T with different methods.

in a real experiment. Therefore, to make the protocol with both high speed and robustness against dissipations, we choose $\lambda = 35/T$, slightly larger than $\overline{\Omega}_0$ ($\overline{\Omega}_0/\lambda \approx 0.3$).

Secondly, since we have adopted a suitable value of the coupling constant λ, we would like to examine the fidelity $F(t)$ and the population $P_m = \langle\varphi_m|\rho(t)|\varphi_m\rangle$ ($m = 1, 2, \cdots, 11$) of state $|\varphi_m\rangle$ during the evolution. The fidelity $F(t)$ versus t/T is plotted in Fig. 4(a). And the the population P_m of each state is shown in Fig. 4(b). As shown in Fig. 4(a), the fidelity $F(t)$ keeps steady during time intervals $[0, 0.3T]$ and $[0.8T, T]$, and increases rapidly to approach 1 during time interval $[0.3T, 0.8T]$. As shown in Fig. 4(b), P_1 falls from 1 to 0 during evolution; P_9, P_{10} and P_{11} are initial 0 and final 1/3 at time $t = T$ as our expectation.

Thirdly, to show that the present protocol is faster than the adiabatic protocol, we plot the fidelity of the target state $|W\rangle$ with different methods versus t/T in Fig. 5. The Rabi frequencies of laser pulses for the STIPAP method can be set as $\Omega_1(t) = \Omega_2(t) = \Omega_3(t) = \sqrt{2}\Omega_a(t)$ and $\Omega_c(t) = \sqrt{2}\Omega_b(t)$, where $\Omega_a(t)$ and $\Omega_b(t)$ are shown in Eq. (15). And it is easy to obtain that $\Omega'_0 = \max_{0 \leq t \leq T}\{\Omega_1(t), \Omega_2(t), \Omega_3(t), \Omega_c(t)\} = \sqrt{2}\Omega_0$. As shown in Fig. 5, the curve of "STAP" describes the change of the fidelity versus t/T of the present protocol, and the curves of "STIRAP" describe the changes of fidelities versus t/T of the STIRAP method under some different conditions. Seen from blue line of Fig. 5, if one use STIRAP method with the same condition as the present protocol ($\Omega'_0 = 12/T$, $\lambda = 35/T$), the final fidelity is only about 0.55 due to the greatly violation of the adiabatic condition. Even when $\Omega'_0 = 35/T$, $\lambda = 100/T$ (see the pink line of Fig. 5) for the STIRAP method, the fidelity can get close to 1, but the result is still a little unsatisfactory. When $\Omega'_0 = 50/T$, $\lambda = 150/T$ (see the green line of Fig. 5) for the STIRAP method, the fidelity can approach 1. However, in this case, the laser amplitude $\Omega'_0 = 50/T$ is much larger than the one ($\overline{\Omega}_0 \approx 12/T$) of the present protocol. If one desire a relative high evolution speed, the product (denotes by μ) of laser amplitude and the evolution time is the smaller the better. Because when two persons have the same value of the laser amplitudes, the one with smaller μ will have less evolution time. Therefore, comparing with the

STIRAP method, the present protocol to obtain a W state is much faster by using multiple Schrödinger dynamics. In addition, it is also been shown in ref. 31 that, to obtain a W state with the adiabatic passage with a fidelity larger that 0.99, the authors should chose $\lambda > 100/T$ and $\Omega_0 = 0.35\lambda$. That supports the discussion here as well.

Fourthly, since the dissipations caused by decoherence mechanisms are ineluctable in real experiments, it is worthwhile to discuss the fidelity $F(t)$ when different kinds of decoherence factors are considered. In the present protocol, the decay of the cavity mode in each CPWR, the energy relaxation and the dephasing of every SQ play the major roles. The evolution of the system can be described by a master equation in Lindblad form as following

$$\dot{\rho} = i[\rho, H_I] + \sum_l \left[L_l \rho L_l^\dagger - \frac{1}{2}(L_l^\dagger L_l \rho + \rho L_l^\dagger L_l) \right],$$

(18)

where, L_l ($l = 1, 2, 3, \ldots, 19$) is the Lindblad operator. There are nineteen Lindblad operators

$$L_1 = \sqrt{\gamma_{1f}} |f\rangle_1 \langle e|, \quad L_2 = \sqrt{\gamma_{2f}} |f\rangle_2 \langle e|, \quad L_3 = \sqrt{\gamma_{3f}} |f\rangle_3 \langle e|, \quad L_4 = \sqrt{\gamma_{cf}} |f\rangle_c \langle e|,$$

$$L_5 = \sqrt{\gamma_{1g}} |g\rangle_1 \langle e|, \quad L_6 = \sqrt{\gamma_{2g}} |g\rangle_2 \langle e|, \quad L_7 = \sqrt{\gamma_{3g}} |g\rangle_3 \langle e|, \quad L_8 = \sqrt{\gamma_{cg}} |g\rangle_c \langle e|,$$

$$L_9 = \sqrt{\kappa_1} a_1, \quad L_{10} = \sqrt{\kappa_2} a_2, \quad L_{11} = \sqrt{\kappa_3} a_3,$$

$$L_{12} = \sqrt{\gamma_{\phi 1f}/2}\,(|e\rangle_1 \langle e| - |f\rangle_1 \langle f|), \quad L_{13} = \sqrt{\gamma_{\phi 2f}/2}\,(|e\rangle_2 \langle e| - |f\rangle_2 \langle f|),$$

$$L_{14} = \sqrt{\gamma_{\phi 3f}/2}\,(|e\rangle_3 \langle e| - |f\rangle_3 \langle f|), \quad L_{15} = \sqrt{\gamma_{\phi cf}/2}\,(|e\rangle_c \langle e| - |f\rangle_c \langle f|),$$

$$L_{16} = \sqrt{\gamma_{\phi 1g}/2}\,(|e\rangle_1 \langle e| - |g\rangle_1 \langle g|), \quad L_{17} = \sqrt{\gamma_{\phi 2g}/2}\,(|e\rangle_2 \langle e| - |g\rangle_2 \langle g|),$$

$$L_{18} = \sqrt{\gamma_{\phi 3g}/2}\,(|e\rangle_3 \langle e| - |g\rangle_3 \langle g|), \quad L_{19} = \sqrt{\gamma_{\phi cg}/2}\,(|e\rangle_c \langle e| - |g\rangle_c \langle g|),$$

(19)

in which γ_{ks} and $\gamma_{\phi ks}$ ($k = 1, 2, 3, s = f, g$) are the energy relaxation rate and dephasing rate of the k-th SQ for decay path $|e\rangle_k \rightarrow |s\rangle_k$, respectively. And γ_{cs} and $\gamma_{\phi cs}$ ($s = f, g$) are the energy relaxation rate and dephasing rate of the SCC qubit for decay path $|e\rangle_c \rightarrow |s\rangle_c$, respectively. κ_k ($k = 1, 2, 3$) is the decay rate of the k-th cavity mode in $CPWR_k$. We suppose $\gamma_{ks} = \gamma, \gamma_{\phi ks} = \gamma_\phi$ ($k = 1, 2, 3, s = f, g$) and $\kappa_k = \kappa$ ($k = 1, 2, 3$) for simplicity. We plot the final fidelity $F(T)$ versus κ/λ and γ/λ in Fig. 6(a), versus κ/λ and γ_ϕ/λ in Fig. 6(b) and versus γ/λ and γ/λ in Fig. 6(c). And we also examine some samples of the final fidelities $F(T)$ with corresponding κ/λ, γ/λ and γ_ϕ/λ and give them in Table 1. As shown in Fig. 6 and Table 1, we can obtain following results. (i) $F(T)$ is insensitive to decays of the cavity modes in CPWRs. This is easy to be understood by seeing Fig. 4(b). Because the populations of $|\varphi_3\rangle$, $|\varphi_4\rangle$ and $|\varphi_5\rangle$ are all almost zero during the whole evolution, the influences from decays of the cavity modes in CPWRs will be greatly resisted. (ii) The fidelity suffers more influence from the energy relaxations of SQs comparing with the influences from decays of the cavity modes in CPWRs. However, $F(T)$ is 0.9502 when $\gamma/\lambda = 0.01, \gamma_\phi/\lambda = 0$ and $\kappa/\lambda = 0$, i.e., the decreasing of $F(T)$ caused by the increasing of γ is only about 0.05. Therefore, the present protocol is also robust against the energy relaxations of SQs. (iii) The dephasing plays a significant role here. When γ_ϕ/λ increases from 0 to 0.001, $F(T)$ decreases from 1 to 0.9824. However, in ref. 31, with the adiabatic passages, the fidelity of the target W state deceases from 1 to 0.85 when γ_ϕ increases only from 0 to 0.0001. This shows that the present protocol is more robust against the dephasing comparing with the adiabatic passages. According to ref. 107, in experiments, parameters $\lambda = 2\pi \times 300$ MHz, $\gamma = 6\pi$ MHZ, $\kappa = 6\pi$ MHz and $\gamma_\phi = 10$ kHz can be realized. By submitting these parameters, we have $F(T) = 0.9484$.

Fifthly, since most of the parameters are hard to faultlessly achieve in experiments, it is necessary to investigate the variations of the parameters caused by the experimental imperfection. Here, we discuss the variation δT of the evolution time T, the variation $\delta \overline{\Omega}_0$ of the laser amplitude $\overline{\Omega}_0$ and the variation $\delta \lambda$ of the coupling constant λ. We plot $F(T')$ versus $\delta T/T$ and $\delta \lambda/\lambda$ in Fig. 7(a), $F(T')$ versus $\delta T/T$ and $\delta \overline{\Omega}_0/\overline{\Omega}_0$ in Fig. 7(b) and $F(T)$ versus $\delta \lambda/\lambda$ and $\delta \overline{\Omega}_0/\overline{\Omega}_0$ in Fig. 7(c), where $T' = T + \delta T$ is the real evolution time when the variation of the evolution time is taken into account. Seen from Fig. 7(a,c), the final fidelity is quite insensitive to the variation $\delta \lambda$. This results has also been announced in Fig. 3. Moreover, according to Fig. 7(a,b), the final fidelity $F(T')$ is very robust against the variation δT. The final fidelity almost unchanged when both $\delta T/T, \delta \lambda/\lambda \leq 10\%$. As shown in Fig. 7(b,c), variation $\delta \overline{\Omega}_0$ influences the final fidelity mainly. However, even when $\delta \overline{\Omega}_0/\overline{\Omega}_0 = 10\%$, the final fidelity is still higher than 0.95. Therefore, we conclude that the present protocol for generating a W state of three SQs is robust against the variations $\delta T, \delta \overline{\Omega}_0$ and $\delta \lambda$.

Sixthly, in experiments, the protocol can be realized in charge qubits and CPWR coupling system. In other words, all the superconducting qubits including the SCC qubit can be chosen to be charge qubits. The structure of the a charge qubit is shown in Fig. 8. As shown in Fig. 8, the charge qubit contains a gate capacitance and two Josephson junctions with Josephson energy E_J. The charge qubit can be manipulated by controlling the gate voltage V_g and the magnetic flux Φ threading the loop. It was pointed out in previous protocols[108,109] that, for a charge qubit with energy structure as Fig. 1(b), when an external applied magnetic flux Φ_x of a pulse threads the ring, it can driven the transition between $|e\rangle \leftrightarrow |f\rangle$, and the Rabi frequency can be given by

$$\Omega(t) = \frac{1}{2L\hbar} \langle f|\Phi|e\rangle \int_S \mathbf{B}_x(\mathbf{r}, t) \cdot d\mathbf{S},$$

(20)

where, L is the loop inductance, S is surface bounded by the loop of the charge qubit, $\mathbf{B}_x(\mathbf{r}, t)$ is the magnetic components of the pulse in the superconducting loop of the charge qubit. For the SQs inside the CPWR, the cavity mode with frequency ω can couples resonantly to the levels $|g\rangle$ and $|e\rangle$ and gives the coupling constant as
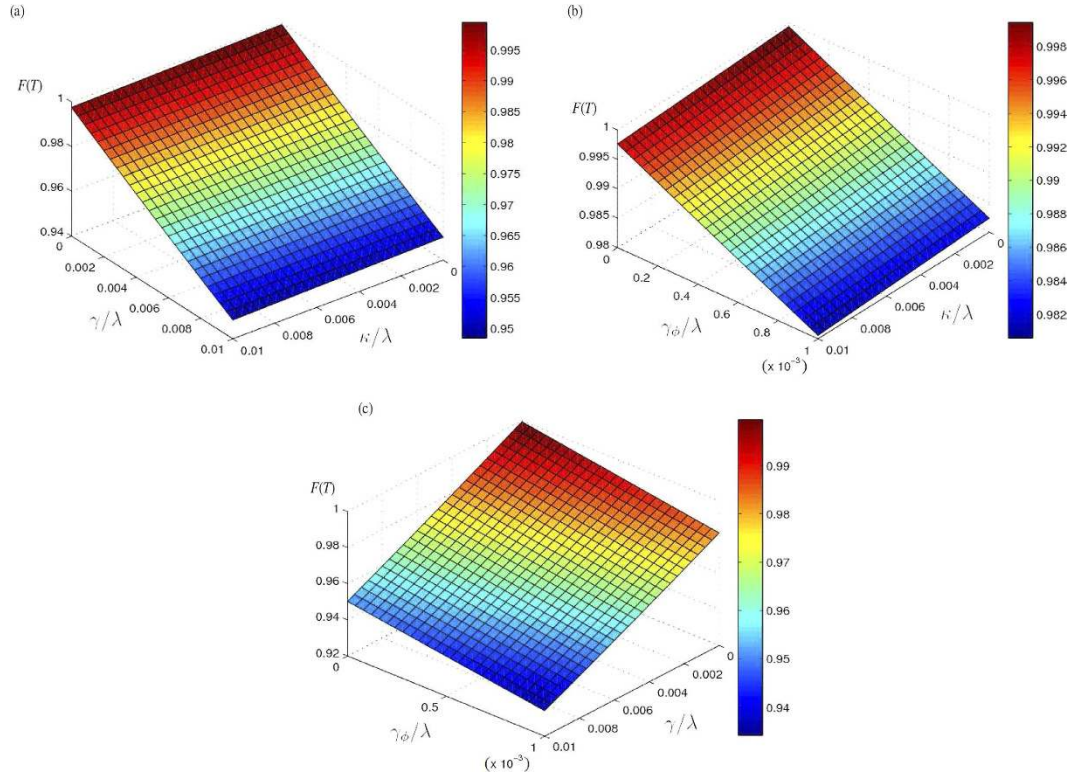
Figure 6. (**a**) The final fidelity $F(T)$ versus κ/λ and γ/λ. (**b**) The final fidelity $F(T)$ versus κ/λ and γ_ϕ/λ. (**c**) The final fidelity $F(T)$ versus γ/λ and γ_ϕ/λ.

$\kappa/\lambda(\times10^{-2})$	$\gamma_\phi/\lambda(\times10^{-3})$	$\gamma/\lambda(\times10^{-2})$	F
1	1	1	0.9325
1	1	0.8	0.9418
1	0.8	1	0.9356
0.8	1	1	0.9328
0.8	0.8	0.8	0.9453
0.8	0.8	0.5	0.9596
0.8	0.5	0.8	0.9502
0.5	0.8	0.8	0.9458
0.5	0.5	0.5	0.9651
0.5	0.5	0.3	0.9749
0.5	0.3	0.5	0.9684
0.3	0.5	0.5	0.9654
0.3	0.3	0.3	0.9786
0.3	0.3	0.1	0.9887
0.3	0.1	0.3	0.9820
0.1	0.3	0.3	0.9790
0.1	0.1	0.1	0.9924

Table 1. Samples of the final fidelities $F(T)$ with corresponding κ/λ, γ/λ and γ_ϕ/λ.

$$\lambda = \frac{1}{L}\sqrt{\frac{\omega}{2\mu_0\hbar}}\,\langle g|\Phi|e\rangle\int_S \mathbf{B}_g(\mathbf{r})\cdot d\mathbf{S},$$

(21)

where, $\mathbf{B}_g(\mathbf{r})$ is the magnetic components of the cavity mode[109,110]. For the SCC qubits placed in the center of the devices, it can couple capacitively to three different CPWR directly. This kind of directly coupling has been shown in many previous protocols both in theory[38,111]. For example, Yang *et al.*[38] have used these kind of coupling to generate entanglement between microwave photons and qubits in multiple cavities coupled by a superconducting
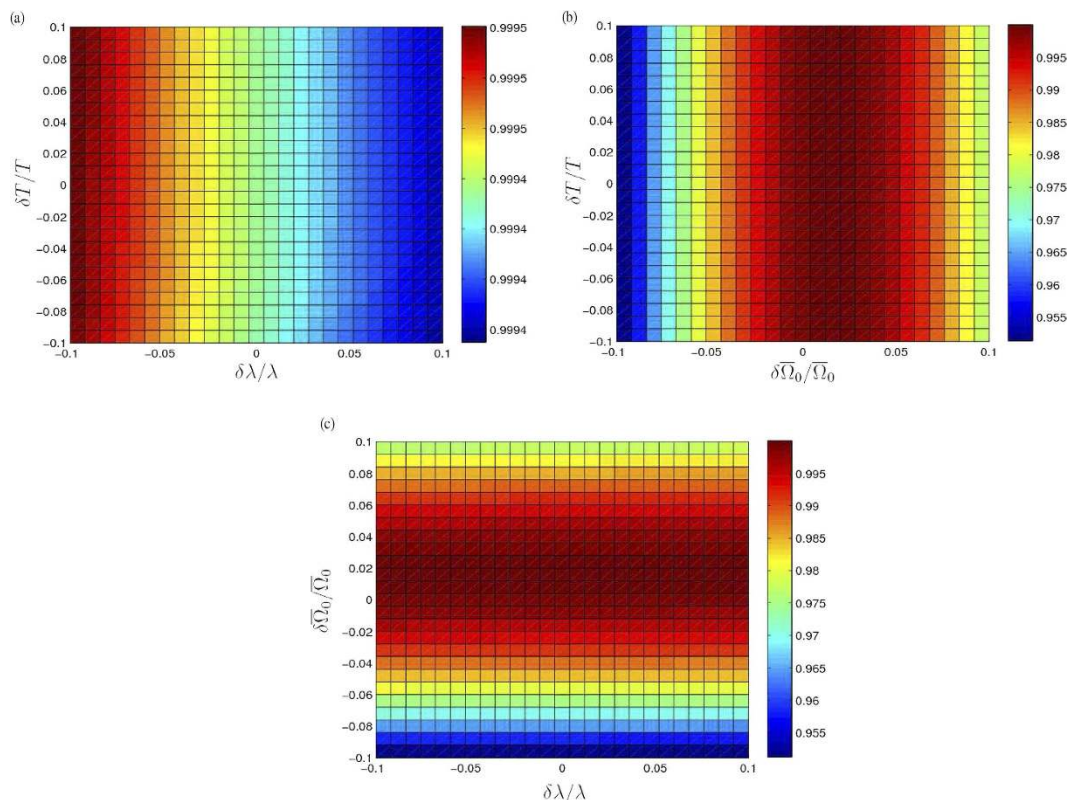
Figure 7. (**a**) The final fidelity $F(T')$ versus $\delta T/T$ and $\delta\lambda/\lambda$. (**b**) The final fidelity $F(T')$ versus $\delta T/T$ and $\delta\overline{\Omega}_0/\overline{\Omega}_0$. (**c**) The final fidelity $F(T)$ versus $\delta\overline{\Omega}_0/\overline{\Omega}_0$ and $\delta\lambda/\lambda$.
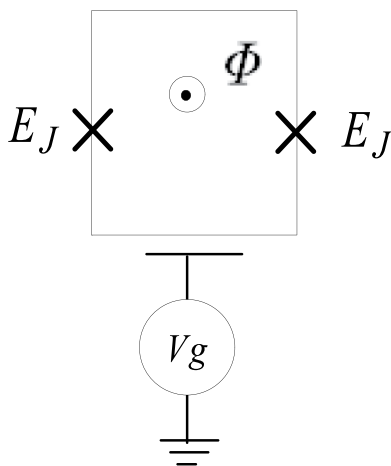

Figure 8. Schematic diagram of a charge qubit.

qubit. Moreover, to improve the efficiency of the coupling between SCC qubit and each CPWR, one can chose SCC qubit to be a transmon[112] or a phase qubit[113] as well.

Conclusions

In conclusion, we have proposed a protocol to generate a W state of three SQs by using multiple Schrödinger dynamics to construct a shortcut to adiabaticity, so that the evolution of the system has been greatly accelerated. Interestingly, the form of the Hamiltonian being designed by the multiple Schrödinger dynamics was the same as that of the system's original Hamiltonian. Therefore, we only need to adjust the Rabi frequencies of laser pulses. In this protocol, the Rabi frequencies of the laser pulses can be expressed by the superpositions of Gaussian functions via the curves fitting. So, the laser pulses can be realized easily in experiments. One the other hand, numerical simulations results have demonstrated that the protocol is robust against different kinds of control parameters

variations and decoherence mechanisms. Notably, the present protocol is more robust against the dephasing, comparing with adiabatic passages. Therefore, we hope the protocol could be controlled and implemented easily in experiments based on a circuit quantum electrodynamics system.

References

1. Barrett, S. D. & Kok, P. Efficient high-fidelity quantum computation using matter qubits and linear optics. *Phys. Rev. A.* **71,** 060310(R) (2005).
2. Lim, Y. L., Barrett, S. D., Beige, A., Kok, P. & Kwek, L. C. Repeat-until-success quantum computing using stationary and flying qubits. *Phys. Rev. A.* **73,** 012304 (2006).
3. Zhou, D. L., Sun, B. & You, L. Generating entangled photon pairs from a cavity-QED system. *Phys. Rev. A* **72,** 040302 (2005).
4. Bennett, C. H. & DiVincenzo, D. P. Quantum information and computation. *Nature (London)* **404,** 247 (2000).
5. Braunstein, S. L. & Kimble, H. J. Teleportation of continuous quantum variables. *Phys. Rev. Lett.* **80,** 869 (1998).
6. Bennett, C. H. & Wiesner, S. J. Communication via one- and two-particle operators on Einstein-Podolsky-Rosen states. *Phys. Rev. Lett.* **69,** 2881 (1992).
7. Ekert, A. K. Quantum cryptography based on Bells theorem. *Phys. Rev. Lett.* **67,** 661 (1991).
8. Divincenzo, D. P. Quantum Computation. *Science* **270,** 255 (1995).
9. Bennett, C. H., Brassard, G., Popescu, S., Schumacher, B., Smolin, J. A. & Wootters, W. K. Purification of noisy entanglement and faithful teleportation via noisy channels. *Phys. Rev. Lett.* **76,** 722 (1996).
10. Sheng, Y. B. & Zhou, L. Two-step complete polarization logic Bell-state analysis. *Sci. Rep.* **5,** 13453 (2016).
11. Zhou, L. & Sheng, Y. B. Complete logic Bell-state analysis assisted with photonic Faraday rotation. *Phys. Rev. A* **92,** 042314 (2015).
12. Zhou, L. & Sheng, Y. B. Feasible logic Bell-state analysis with linear optics. *Sci. Rep.* **6,** 20901 (2016).
13. Bell, J. S. On the einstein podolsky rosen paradox. *Physics (Long Island City, NY)* **1,** 195 (1965).
14. Dür, W., Vidal, G. & Cirac, J. I. Three qubits can be entangled in two inequivalent ways. *Phys. Rev. A* **62,** 062314 (2000).
15. Greenberger, D. M., Horne, M. A. & Zeilinger, A. Going beyond Bell's theorem. In Bell's theorem, quantum theory, and conceptions of the universe, edited by Kafatos, M. (Kluwer, Dordrecht) p. 69 (1989).
16. Li, X. H., Deng, F. G. & Zhou, H. Y. Improving the security of secure direct communication based on the secret transmitting order of particles. *Phys. Rev. A* **74,** 054302 (2006).
17. Wang, C., Deng, F. G., Li, Y. S., Liu, X. S. & Long, G. L. Quantum secure direct communication with high-dimension quantum superdense coding. *Phys. Rev. A* **71,** 044305 (2005).
18. Xiao, L., Long, G. L., Deng, F. G. & Pan, J. W. Efficient multiparty quantum-secret-sharing schemes. *Phys. Rev. A* **69,** 052307 (2004).
19. Hillery, M., Bužek, V. & Berthiaume, A. Quantum secret sharing. *Phys. Rev. A* **59,** 1829 (1999).
20. Bennett, C. H., Brassard, G., Crepeau, C., Jozsa, R., Peres, A. & Wootters, W. K. Teleporting an unknown quantum state via dual classical and Einstein-Podolsky-Rosen channels. *Phys. Rev. Lett.* **70,** 1895 (1993).
21. Karlsson, A. & Bourennane, M. Quantum teleportation using three-particle entanglement. *Phys. Rev. A* **58,** 4394 (1998).
22. Bužek, V. & Hillery, M. Crossed-field hydrogen atom and the three-body Sun-Earth-Moon problem. *Phys. Rev. A* **54,** 1884 (1996).
23. Gisin, N. & Massar, S. Optimal quantum cloning machines. *Phys. Rev. Lett.* **79,** 2153 (1997).
24. Chen, Y. H., Huang, B. H., Song, J. & Xia, Y. Transitionless-based shortcuts for the fast and robust generation of W states. *Opt. Comm.* **380,** 140 (2016).
25. An, N. B. Cavity-catalyzed deterministic generation of maximal entanglement between nonidentical atoms. *Phys. Lett. A* **344,** 77 (2005).
26. Zheng, S. B. Scalable generation of multi-atom W states with a single resonant interaction. *J. Opt. B* **7,** 10 (2005).
27. Kang, Y. H., Xia, Y. & Lu, P. M. Effective scheme for preparation of a spin-qubit Greenberger-Horne-Zeilinger state and W state in a quantum-dot-microcavity system. *J. Opt. Soc. Am. B* **32,** 1323 (2015).
28. Eibl, M., Kiesel, N., Bourennane, M., Kurtsiefer, C. & Weinfurter, H. Experimental Realization of a Three-Qubit Entangled W State. *Phys. Rev. Lett.* **92,** 077901 (2004).
29. Zou, X. B., Pahlke, K. & Mathis, W. Generation of an entangled four-photon W state. *Phys. Rev. A* **66,** 044302 (2002).
30. Neeley, M., Bialczak, R. C., Lenander, M. & Lucero, E. Generation of three-qubit entangled states using superconducting phase qubits. *Nature (London)* **467,** 570 (2010).
31. Wei, X. & Chen, M. F. Preparation of multi-qubit W states in multiple resonators coupled by a superconducting qubit via adiabatic passage. *Quantum Inf. Process.* **14,** 2419 (2015).
32. Wei, X. & Chen, M. F. Generation of N-qubit W state in N separated resonators via resonant interaction. *Int. J. Theor. Phys.* **54,** 812 (2015).
33. Helmer, F. & Marquardt, F. Measurement-based synthesis of multiqubit entangled states in superconducting cavity QED. *Phys. Rev. A* **79,** 052328 (2009).
34. Song, K. H., Zhou, Z. W. & Guo, G. C. Quantum logic gate operation and entanglement with superconducting quantum interference devices in a cavity via a Raman transition. *Phys. Rev. A* **71,** 052310 (2005).
35. Deng, Z. J., Gao, K. L. & Feng, M. Generation of N-qubit W states with rf SQUID qubits by adiabatic passage. *Phys. Rev. A* **74,** 064303 (2006).
36. Wu, J. L., Song, C., Xu, J., Yu, L., Ji, X. & Zhang, S. Adiabatic passage for one-step generation of n-qubit Greenberger-Horne-Zeilinger states of superconducting qubits via quantum Zeno dynamics. *Quantum Inf. Process.*, doi: 10.1007/s11128-016-1366-0.
37. You, J. Q. & Nori, F. Atomic physics and quantum optics using superconducting circuits. *Nature (London)* **474,** 589 (2011).
38. Yang, C. P., Su, Q. P., Zheng, S. B. & Han, S. Generating entanglement between microwave photons and qubits in multiple cavities coupled by a superconducting qutrit. *Phys. Rev. A* **87,** 022320 (2013).
39. Clarke, J. & Wilhelm, F. K. Superconducting quantum bits. *Nature (London)* **453,** 1031 (2008).
40. Filipp, S., Maurer, P., Leek, P. J., Baur, M., Bianchetti, R., Fink, J. M., Göppl, M., Steffen, L., Gambetta, J. M., Blais, A. & Wallraff, A. Two-qubit state tomography using a joint dispersive readout. *Phys. Rev. Lett.* **102,** 200402 (2009).
41. Bialczak, R. C., Ansmann, M., Hofheinz, M., Lucero, E., Neeley, M., O'Connell, A. D., Sank, D., Wang, H., Wenner, J., Steffen, M., Cleland, A. N. & Martinis, J. M. Quantum process tomography of a universal entangling gate implemented with Josephson phase qubits. *Nat. Phys.* **6,** 409 (2010).
42. Yamamoto, T., Neeley, M., Lucero, E., Bialczak, R. C., Kelly, J., Lenander, M., Mariantoni, M., O'Connell, A. D., Sank, D., Wang, H., Weides, M., Wenner, J., Yin, Y., Cleland, A. N. & Martinis, J. M. Quantum process tomography of two-qubit controlled-Z and controlled-NOT gates using superconducting phase qubits. *Phys. Rev. B* **82,** 184515 (2010).
43. Reed, M. D., DiCarlo, L., Johnson, B. R., Sun, L., Schuster, D. I., Frunzio, L. & Schoelkopf, R. J. High-fidelity readout in circuit quantum electrodynamics using the Jaynes-Cummings nonlinearity. *Phys. Rev. Lett.* **105,** 173601 (2010).
44. Yang, C. P., Chu, S. I. & Han, S. Possible realization of entanglement, logical gates, and quantum-information transfer with superconducting-quantum-interference-device qubits in cavity QED. *Phys. Rev. A* **67,** 042311 (2003).
45. Majer, J., Chow, J. M., Gambetta, J. M., Koch, J., Johnson, B. R., Schreier, J. A., Frunzio, L., Schuster, D. I., Houck, A. A., Wallraff, A., Blais, A., Devoret, M. H., Girvin, S. M. & Schoelkopf, R. J. Coupling superconducting qubits via a cavity bus. *Nature (London)* **449,** 443 (2007).

46. DiCarlo, L., Chow, J. M., Gambetta, J. M., Bishop, L. S., Johnson, B. R., Schuster, D. I., Majer, J., Blais, A., Frunzio, L., Girvin, S. M. & Schoelkopf, R. J. Demonstration of two-qubit algorithms with a superconducting quantum processor. *Nature (London)* **460,** 240 (2009).
47. Blais, A., Huang, R. S., Wallraff, A., Girvin, S. M. & Schoelkopf, R. J. Cavity quantum electrodynamics for superconducting electrical circuits: An architecture for quantum computation. *Phys. Rev. A* **69,** 062320 (2004).
48. Yang, C. P., Chu, S. I. & Han, S. Quantum information transfer and entanglement with SQUID qubits in cavity QED: a dark-state scheme with tolerance for nonuniform device parameter. *Phys. Rev. Lett.* **92,** 117902 (2004).
49. Wallraff, A., Schuster, D. I., Blais, A., Frunzio, L., Huang, R. S., Majer, J., Kumar, S., Girvin, S. M. & Schoelkopf, R. J. Strong coupling of a single photon to a superconducting qubit using circuit quantum electrodynamics. *Nature (London)* **431,** 162 (2004).
50. Chiorescu, I., Bertet, P., Semba, K., Nakamura, Y., Harmans, C. J. P. M. & Mooij, J. E. Coherent dynamics of a flux qubit coupled to a harmonic oscillator. *Nature (London)* **431,** 159 (2004).
51. Fewell, M. P., Shore, B. W. & Bergmann, K. Coherent population transfer among three states: full algebraic solutions and the relevance of non adiabatic processes to transfer by delayed pulses. *Aust. J. Phys.* **50,** 281 (1997).
52. Bergmann, K., Theuer, H. & Shore, B. W. Coherent population transfer among quantum states of atoms and molecules. *Rev. Mod. Phys.* **70,** 1003 (1998).
53. Vitanov, N. V., Halfmann, T., Shore, B. W. & Bergmann, K. Laser-induced population transfer by adiabatic passage techniques. *Annu. Rev. Phys. Chem.* **52,** 763 (2001).
54. Král, P., Thanopulos, I. & Shapiro, M. Coherently controlled adiabatic passage. *Rev. Mod. Phys.* **79,** 53 (2007).
55. Demirplak, M. & Rice, S. A. Adiabatic population transfer with control fields. *J. Phys. Chem. A* **107,** 9937 (2003).
56. Demirplak, M. & Rice, S. A. On the consistency, extremal, and global properties of counterdiabatic fields. *J. Chem. Phys.* **129,** 154111 (2008).
57. Torrontegui, E., Ibáñez, S., Martnez-Garaot, S., Modugno, M., del Campo, A., Gué-Odelin, D., Ruschhaupt, A., Chen, X. & Muga, J. G. Shortcuts to adiabaticity. *Adv. Atom. Mol. Opt. Phys.* **62,** 117 (2013).
58. Berry, M. V. Transitionless quantum driving. *J. Phys. A* **42,** 365303 (2009).
59. Chen, X., Lizuain, I., Ruschhaupt, A., Guéry-Odelin, D. & Muga, J. G. Shortcut to adiabatic passage in two- and three-level atoms. *Phys. Rev. Lett.* **105** 123003 (2010).
60. del Campo, A. Shortcuts to adiabaticity by counterdiabatic driving. *Phys. Rev. Lett.* **111,** 100502 (2013).
61. Chen, X., Torrontegui, E. & Muga, J. G. Lewis-Riesenfeld invariants and transitionless quantum driving. *Phys. Rev. A* **83,** 062116 (2011).
62. Muga, J. G., Chen, X., Ruschhaup, A. & Guéry-Odelin, D. Frictionless dynamics of Bose-Einstein condensates under fast trap variations. *J. Phys. B* **42,** 241001 (2009).
63. Chen, X. *et al.* Fast optimal frictionless atom cooling in harmonic traps: shortcut to adiabaticity. *Phys. Rev. Lett.* **104,** 063002 (2010).
64. Torrontegui, E., Ibáñez, S., Chen, X., Ruschhaupt, A., Guéry-Odelin, D. & Muga, J. G. Fast atomic transport without vibrational heating. *Phys. Rev. A* **83,** 013415 (2011).
65. Muga, J. G., Chen, X., Ibáñez, S., Lizuain, I. & Ruschhaupt, A. Transitionless quantum drivings for the harmonic oscillator. *J. Phys. B* **43,** 085509 (2010).
66. Torrontegui, E., Chen, X., Modugno, M., Ruschhaupt, A., Guéry-Odelin, D. & Muga, J. G. Fast transitionless expansion of cold atoms in optical Gaussian-beam traps. *Phys. Rev. A* **85,** 033605 (2012).
67. Masuda, S. & Nakamura, K. Acceleration of adiabatic quantum dynamics in electromagnetic fields. *Phys. Rev. A* **84,** 043434 (2011).
68. Masuda, S. & Rice, S. A. Fast-Forward Assisted. *STIRAP. J. Phys. Chem. A.* **199,** 3479 (2015).
69. Chen, Y. H., Xia, Y., Chen, Q. Q. & Song, J. Fast and noise-resistant implementation of quantum phase gates and creation of quantum entangled states. *Phys. Rev. A* **91,** 012325 (2015).
70. Chen, X. & Muga, J. G. Transient energy excitation in shortcuts to adiabaticity for the time-dependent harmonic oscillator. *Phys. Rev. A* **82,** 053403 (2010).
71. Schaff, J. F., Capuzzi, P., Labeyrie, G. & Vignolo, P. Shortcuts to adiabaticity for trapped ultracold gases. *New J. Phys.* **13,** 113017 (2011).
72. Chen, X., Torrontegui, E., Stefanatos, D., Li, J. S. & Muga, J. G. Optimal trajectories for efficient atomic transport without final excitation. *Phys. Rev. A* **84,** 043415 (2011).
73. Torrontegui, E., Chen, X., Modugno, M., Schmidt, S., Ruschhaupt, A. & Muga, J. G. Fast transport of Bose-Einstein condensates. *New J. Phys.* **14,** 013031 (2012).
74. del Campo, A. Frictionless quantum quenches in ultracold gases: A quantum-dynamical microscope. *Phys. Rev. A* **84,** 031606(R) (2011).
75. del Campo, A. Fast frictionless dynamics as a toolbox for low-dimensional Bose-Einstein condensates. *Eur. Phys. Lett.* **96,** 60005 (2011).
76. Ruschhaupt, A., Chen, X., Alonso, D. & Muga, J. G. Optimally robust shortcuts to population inversion in two-level quantum systems. *New J. Phys.* **14,** 093040 (2012).
77. Schaff, J. F., Song, X. L., Vignolo, P. & Labeyrie, G. Fast optimal transition between two equilibrium states. *Phys. Rev. A* **82,** 033430 (2010).
78. Schaff, J. F., Song, X. L., Capuzzi, P., Vignolo, P. & Labeyrie, G. Shortcut to adiabaticity for an interacting Bose-Einstein condensate. *Eur. Phys. Lett.* **93,** 23001 (2011).
79. Chen, X. & Muga, J. G. Engineering of fast population transfer in three-level systems. *Phys. Rev. A* **86,** 033405 (2012).
80. Chen, Z., Chen, Y. H., Xia, Y., Song, J. & Huang, B. H. Fast generation of three-atom singlet state by transitionless quantum driving. *Sci. Rep.* **6,** 22202 (2016).
81. Lu, M., Xia, Y., Shen, L. T., Song, J. & An, N. B. Shortcuts to adiabatic passage for population transfer and maximum entanglement creation between two atoms in a cavity. *Phys. Rev. A* **89,** 012326 (2014).
82. Chen, Y. H., Xia, Y., Chen, Q. Q. & Song, J. Efficient shortcuts to adiabatic passage for fast population transfer in multiparticle systems. *Phys. Rev. A* **89,** 033856 (2014).
83. Song, X. K., Zhang, H., Ai, Q., Qiu, J. & Deng, F. G. Shortcuts to adiabatic holonomic quantum computation in decoherence-free subspace with transitionless quantum driving algorithm. *New J. Phys.* **18,** 023001 (2016).
84. Vacanti, G., Fazio, R., Montangero, S., Palma, G. M., Paternostro, M. & Vedral, V. Transitionless quantum driving in open quantum systems. *New J. Phys.* **16,** 053017 (2016).
85. Santos, A. C. & Sarandy, M. S. Superadiabatic controlled evolutions and universal quantum computation. *Sci. Rep.* **5,** 15775 (2015).
86. Santos, A. C., Silva, R. D. & Sarandy, M. S. Shortcut to adiabatic gate teleportation. *Phys. Rev. A* **93,** 012311 (2016).
87. Hen, I. Quantum gates with controlled adiabatic evolutions. *Phys. Rev. A* **91,** 022309 (2015).
88. Sarandy, M. S., Wu, L. A. & Lidar, D. Consistency of the adiabatic theorem. *Quantum Inf. Process* **3,** 331 (2004).
89. Coulamy, I. B., Santos, A. C., Hen, I. & Sarandy, M. S. Energetic cost of superadiabatic quantum computation. arXiv:1603.07778.
90. Rams, M. M., Mohseni, M. & del Campo, A. Inhomogeneous quasi-adiabatic driving of quantum critical dynamics in weakly disordered spin chains. arXiv:1606.07740.
91. Deffner, S., Jarzynski, C. & del Campo, A. Classical and quantum shortcuts to adiabaticity for scale-invariant driving. *Phys. Rev. X* **4,** 021013 (2014).

92. del Campo, A. Shortcuts to adiabaticity in quantum many-body systems: a quantum dynamical microscope. *Aps March Meeting* (2014).
93. Huang, B. H., Chen, Y. H., Wu, Q. C., Song, J. & Xia, Y. Fast generating Greenberger-Horne-Zeilinger state via iterative interaction pictures. *Laser Phys. Lett.* **13,** 105202 (2016).
94. Chen, Y. H., Xia, Y., Song, J. & Chen, Q. Q. Shortcuts to adiabatic passage for fast generation of Greenberger-Horne-Zeilinger states by transitionless quantum driving. *Sci. Rep.* **5,** 15616 (2016).
95. Huang, X. B., Zhong, Z. R. & Chen, Y. H. Generation of multi-atom entangled states in coupled cavities via transitionless quantum driving. *Quantum Inf. Process.* **14,** 4775 (2015).
96. Shan, W. J., Xia, Y., Chen, Y. H. & Song, J. Fast generation of N-atom Greenberger-Horne-Zeilinger state in separate coupled cavities via transitionless quantum driving. *Quantum Inf. Process.* **15,** 2359 (2016).
97. Martnez-Garaot, S., Torrontegui, E., Chen, X. & Muga, J. G. Shortcuts to adiabaticity in three-level systems using Lie transforms. *Phys. Rev. A* **89,** 053408 (2014).
98. Opatrný, T. & Mømer, K. Partial suppression of nonadiabatic transitions. *New J. Phys.* **16,** 015025 (2014).
99. Saberi, H., Opatrny, T., Mømer, K. & del Campo, A. Adiabatic tracking of quantum many-body dynamics. *Phys. Rev. A* **90,** 060301(R) (2014).
100. Torrontegui, E., Martnez-Garaot, S. & Muga, J. G. Hamiltonian engineering via invariants and dynamical algebra. *Phys. Rev. A* **89,** 043408 (2014).
101. Torosov, B. T., Valle, G. D. & Longhi, S. Non-Hermitian shortcut to adiabaticity. *Phys. Rev. A* **87,** 052502 (2013).
102. Torosov, B. T., Valle, G. D. & Longhi, S. Non-Hermitian shortcut to stimulated Raman adiabatic passage. *Phys. Rev. A* **89,** 063412 (2014).
103. Chen, Y. H., Wu, Q. C., Huang, B. H., Xia, Y. & Song, J. Method for constructing shortcuts to adiabaticity by a substitute of counterdiabatic driving terms. *Phys. Rev. A* **93,** 052109 (2016).
104. Ibáñez, S., Chen, X. & Muga, J. G. Improving shortcuts to adiabaticity by iterative interaction pictures. *Phys. Rev. A* **87,** 043402 (2013).
105. Ibáñez, S., Chen, X., Torrontegui, E., Muga, J. G. & Ruschhaupt, A. Multiple Schrödinger pictures and dynamics in shortcuts to adiabaticity. *Phys. Rev. Lett.* **109,** 100403 (2012).
106. Song, X. K., Ai, Q., Qiu, J. & Deng, F. G. Physically feasible three-level transitionless quantum driving with multiple Schröodinger dynamics. *Phys. Rev. A* **93,** 052324 (2016).
107. Kang, Y. H., Chen, Y. H., Wu, Q. C., Huang, B. H., Xia, Y. & Song, J. Reverse engineering of a Hamiltonian by designing the evolution operators. *Sci. Rep.* **6,** 30151 (2016).
108. Xiang, Z. L., Ashhab, S., You, J. Q. & Nori, F. Hybrid quantum circuits: superconducting circuits interacting with other quantum systems. *Rev. Mod. Phys.* **85,** 623 (2013).
109. Siewert, J., Brandes, T. & Falci, G. Adiabatic passage with superconducting nanocircuits. *Opt. Commun.* **264,** 435 (2006).
110. Feng, Z. B. Coupling charge qubits via Raman transitions in circuit QED. *Phys. Rev. A* **78,** 032325 (2008).
111. Strauch, F. W., Jacobs, K. & Simmonds, R. W. Arbitrary Control of Entanglement between two Superconducting Resonators. *Phys. Rev. Lett.* **105,** 050501 (2010).
112. Koch, J., Yu, T. M., Gambetta, J., Houck, A. A., Schuster, D. I., Majer, J., Blais, A., Devoret, M. H., Girvin, S. M. & Schoelkopf, R. J. Charge-insensitive qubit design derived from the Cooper pair box. *Phys. Rev. A* **76,** 042319 (2007).
113. Mariantoni, M., Wang, H., Bialczak, R. C., Lenander, M., Lucero, E., Neeley, M., O'Connell, A. D., Sank, D., Weides, M., Wenner, J., Yamamoto, T., Yin, Y., Zhao, J., Martinis, J. M. & Cleland, A. N. Photon shell game in three-resonator circuit quantum electrodynamics. *Nature Physics* **7,** 287 (2011).

Acknowledgements

Author Contributions

Y.X. and Y.H.K. came up with the initial idea for the work and performed the simulations for the model. Y.H.C., Q.C.W., J.S. and B.H.H. performed the calculations for the model. Y.X., Y.H.K. and Y.H.C. performed all the data analysis and the initial draft of the manuscript. All authors participated in the writing and revising of the text.

Additional Information

Competing financial interests: The authors declare no competing financial interests.

How to cite this article: Kang, Y.-H. *et al.* Fast generation of W states of superconducting qubits with multiple Schrödinger dynamics. *Sci. Rep.* **6**, 36737; doi: 10.1038/srep36737 (2016).

Publisher's note: Springer Nature remains neutral with regard to jurisdictional claims in published maps and institutional affiliations.